Role of PTA in the prevention of Cu(Amyloid-β) induced ROS formation and Amyloid-β oligomerisation in the presence of Zn

Elena Atrián-Blasco, Elena Cerrada, Peter Faller, M. Laguna, Christelle Hureau

Role of PTA in the prevention of Cu(Amyloid-β) induced ROS formation and Amyloid-β oligomerisation in the presence of Zn

Elena Atrián-Blasco,a,b Elena Cerrada,b Peter Faller,a,c Mariano Laguna,b and Christelle Hureau,*a

[a] LCC-CNRS, Université de Toulouse, CNRS, 31400 Toulouse, France.
E-mail : christelle-hureau@lcc-toulouse.fr
[b] Instituto de Síntesis Química y Catálisis Homogénea, Universidad de Zaragoza-CSIC, Pza. San Francisco s/n, 50009 Zaragoza, Spain.
[c] Biometals and Biological Chemistry, Institut de Chimie, UMR 7177, Université de Strasbourg, CNRS, Le Bel, 4 rue B. Pascal, 67081 Strasbourg, France.

Metal-targeting drugs are being widely explored as a possible treatment of Alzheimer's disease, but most of these ligands are developed to coordinate Cu(II). In a previous communication (*Metallomics*, 2015, 7, 1229) we have shown another strategy where Cu(I) was targeted with the PTA (1,3,5-triaza-7-phosphaadamantane) ligand that is in addition able to target Cu(II) as well, reduce it and keep it in a safe complexed species. Removal of Cu(II) from the amyloid-β peptide prevents the stabilization of oligomers and protofibrils and the complexation of Cu(I) also stops the formation of reactive oxygen species. Besides, the presence of zinc, which is found in the synaptic cleft in higher concentration than copper, can hamper the ability of metal-targeting drug candidates, an issue that is still poorly considered and studied. Here we show that PTA fully keeps the above described properties even in presence of zinc, thus fulfilling an additional pre-requisite for its use as a model of Cu(I)-targetting drug candidates in the Alzheimer's disease context.

Introduction

Alzheimer's disease (AD) is the leading cause of dementia in the elderly affecting nearly 47 million people worldwide.1 The underlying mechanisms of this complex disorder are not clear, but there is evidence and a relatively wide agreement that the so-called amyloid cascade is a key and early event in the development of AD. This hypothesis proposes an increased extracellular accumulation of the peptide amyloid-β (Aβ) and subsequent aggregation into fibrils found in amyloid plaques, a post-mortem hallmark of AD.2 The mis-metabolism of Aβ has been suggested to be the initiating event in AD pathogenesis. Formation of Aβ aggregates would instigate further pathological events, including the formation of intracellular neurofibrillary tangles of Tau protein (the other hallmark of AD), disruption of synaptic connections and ultimately neuronal cells death and dementia.

In vitro and in vivo studies indicate that metal ions, mainly Cu, Zn and Fe ions are involved in AD.3,4 In particular, the concentration of metal ions in the senile plaques is higher than in cerebrospinal fluid (mM versus μM).5 There is even evidence that the binding of metal ions to Aβ is required for aggregation at physiological concentrations.6 Cu and Zn ions can both bind to Aβ,7 while there is no strong evidence of Fe binding to Aβ.3,8 Cu and Zn modulate Aβ aggregation both with respect to the kinetics and mechanisms of aggregation and the morphology of the formed aggregates.9,10 Based on in vitro experiments, it has been proposed that Cu can stabilize metastable oligomeric species considered as the most toxic ones,11–13 while Zn induces the formation of weakly-structured

aggregates.13–18 However, results from in vitro experiments also mainly depend on the ratio of metal ions per peptide, a parameter that is not fully known under AD conditions.7,18 Due to its redox ability, Cu ions participate in the formation of Reactive Oxygen Species (ROS) contributing to the oxidative stress implicated in AD.19 Therefore disrupting the extracellular Aβ/Cu interaction and restoring the Cu homeostasis using synthetic ligands remains a promising therapeutic strategy.20 When Cu is regarded as the therapeutic target, Cu(II) has been preferred over Cu(I) although the extra-cellular space in brain is reductive (the ascorbate concentration in the extracellular fluid in the brain is estimated between 200 and 400 µM), 21,22 and the ability of the Amyloid Precursor Protein to reduce the Cu(II).23

Cu dysmetabolism was also reported in other neurological diseases like prion diseases, motor neuron diseases and Parkinson's disease.24–25 Cu is an essential metal ion26 and, in the case of neurons, this is strengthened by the fact that neurological disturbances are hallmarks of the congenital diseases of Cu metabolism, such Menkes' (accumulation of Cu) and Wilson's (lack of Cu).27 Furthermore, it was found that, when in the synaptic cleft, Cu can control the activity of neurotransmitter receptors, thus affecting excitability. These aspects reinforce the importance of the maintenance of Cu homeostasis for nervous system physiology.28

Cu(I/II) and/or Zn(II) do bind to the Aβ peptide, with the following properties (figure 1): (i) Two Cu(II)-Aβ species coexist near physiological pH with a main component (noted I) where Cu(II) is bound by the N-terminal amine, the adjacent carbonyl function and two imidazole rings from His6 and His13 or His14. In the minor component (noted II), the Asp1-Ala2 peptide bond is deprotonated and bound to the Cu(II). This induces the coordination of the adjacent carbonyl function. The last equatorial position is occupied by an imidazole ring from one of the three His residues, with no strong preference for one His residue.4,7 The most consensual value for the conditional affinity of Cu(II) to Aβ is 10^{10} M^{-1} at pH 7.4.[29,30] (ii) Regarding Zn, the coordination is made by two His and two carboxylic acid residues, with a main contribution from His6 and Glu11 and is the predominant species around pH 7.4.[7,31] Conditional affinity is about 4 to 5 orders of magnitude weaker compared to Cu(II) at pH 7.4.[32] (iii) Cu(I) is bound by imidazole rings from two among the three His residues in a linear disposition.[3,33,34] The affinity for Cu(I) is still controversial, with values between 10^{7} M^{-1} and 10^{10} M^{-1} reported in the literature.[30,35,36] (iv)

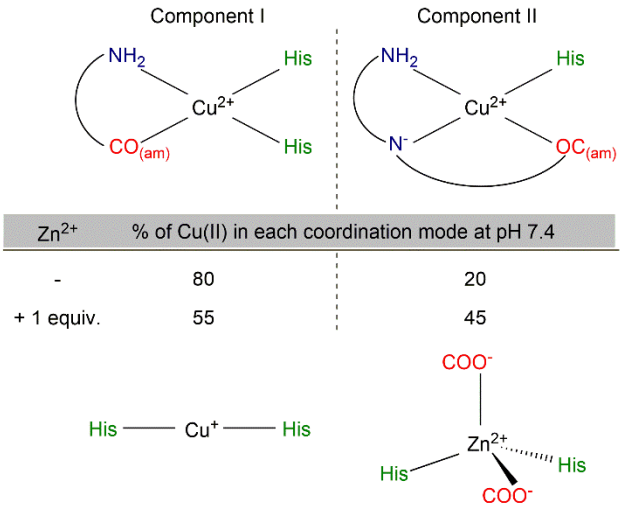

Figure 1. Proposed Cu(II) (upper), Cu(I) (bottom left) and Zn(II) (bottom right) coordination to Aβ at physiological pH. Values of % of Cu(II) are given from ref. 6.

hetero-bimetallic species have also been observed and spectroscopically characterized. For Cu^{II},Zn(Aβ),

the co-presence of Zn induces a shift of Cu(II) towards the component II site, while Zn may keep two imidazole rings from the remaining His and two carboxylates. For Cu^{I},Zn(Aβ), the Cu(I) site is identical as in absence of Zn (figure 1), and the Zn site may accordingly change significantly with the possibility to keep only one imidazole ring from His.[37,38] Given the different coordination geometries of Cu(II) and Cu(I) bound to the peptide, the redox properties of the Cu(Aβ) species are every complex. The electron transfer is sluggish, proceeding via a low populated highly redox-active state in equilibrium with the two Cu(I)(Aβ) and Cu(II)(Aβ) spectroscopically characterized.[39] This so-called "in-between" state is also responsible of the production of ROS.[40]

Despite all the broad research undergone on the bioinorganic aspect of Alzheimer's disease in the last years, there is still no clear evidence of the in vivo metal-binding to Aβ beyond its presence in aggregates.[4,41] Nevertheless, the metal hypothesis in link to the amyloid cascade proposes that weakly-bound metal ions from extracellular pools, especuially those released in the synaptic cleft, could interact with Aβ peptide.[25,42] From this interaction, a modulation of the aggregation of the peptide and a redox activity of the Cu-peptide complex have been hypothesised with different degrees of implication in the development of Alzheimer's disease.

Different strategies have been considered and studied for the treatment of AD, many of them focussed in the amyloid cascade hypothesis and its implication on the development of the disease. Given the potential impact of metal ions in AD the production of metal-coordinating ligands, and more specifically Cu-targeting molecules can be found among these strategies.[20] Two examples of these molecules are clioquinol and PBT2, ligands that made up to Phase II clinical trials but failed in this step.[43] Current attempts at regulating Cu levels in AD might not have been successful for several reasons: (i) keeping Cu(II) as the sole target and (ii) the poor selectivity between Cu and Zn of the proposed molecules given that Zn concentration within the synaptic clefts where the amyloid cascade occurs is much higher than Cu: up to 350 µM for zinc[44] and in the 10-100 µM range for copper.[45,46] With respect to Cu(I), reaching an appropriate Cu(I) over Zn(II) selectivity mainly relies on the nature of the ligand (rather than on geometrical constraints as for Cu(II)). Since Cu(I) is a softer acid than Zn(II) according to the HSAB theory,[47] softer base ligands such as S and P ligands will prefer Cu(I) over Zn(II) binding. Hence, the PTA (PTA = 1,3,5-triaza-7-phosphaadamantane) ligand previously studied for its ability to remove either Cu(I) or Cu(II) (after reduction) from Aβ and stop associated ROS formation and prevent Cu(II) modulation of Aβ aggregation,[48] should fulfil this selectivity requirement.

PTA is a cage-like water-soluble air-stable monodentate phosphine ligand with properties suitable for medicinal applications, especially the ability to solubilize transition metal complexes with anti-tumour activity.[49] Since PTA is a monodentate ligand, it can form up to 4 different species with Cu(I): $[Cu(PTA)_n]^+$ (n = 1–4). Thus, depending on the concentration and Cu(I):PTA stoichiometry, the predominant species differs.[48,50,51]

In the present work, we report the use of PTA in presence of Zn (and in absence for direct comparison) on Cu(I) (and Cu(II)) targeting, removal from Aβ, and consequences on ROS production and Aβ aggregation, the two key and deleterious events occurring in the amyloid cascade linked to the aetiology of AD. This is a proof-of-concept study in the sense that it addresses the possibility to keep in the presence of Zn the positive effect of PTA[48] against Cu-associated deleterious effects such as ROS production and oligomers formation. Nevertheless, other requirements the ligand should also fulfil for

further therapeutic purposes such as the capacity to pass through the blood-brain barrier[52] or to have a good ADME (absorption, distribution, metabolism and excretion) / Toxicity profile[53] are not under focus.

Experimental

Chemicals

A stock solution of Cu(II) at 20 mM was prepared by dissolving $CuSO_4 \cdot 5H_2O$ (Sigma Aldrich) in ultrapure water. Similarly, $ZnSO_4 \cdot H_2O$ (from Strem Chemicals) was dissolved in ultrapure water to prepare a 20 mM stock solution of Zn(II). HEPES buffer was bought from Sigma Aldrich and dissolved in ultrapure water to a final concentration of 0.5 M, and pH was adjusted to 7.4 by addition of NaOH. A 0.5 M stock solution of Tris-d11 was prepared by dissolving the appropriate amount of the buffer powder (Sigma Aldrich) in D_2O and adjusting the pH with D_2SO_4. A stock solution of sodium ascorbate (Sigma Aldrich) at 10 mM was daily prepared in ultrapure water. PTA was prepared as previously described in the literature.[54] A stock solution of Thioflavin T (Acros Organics) at ca. 5 mM was prepared by dissolving the powder in ultrapure water, with further titration by UV-vis spectroscopy (ε_{412}-ε_{500} = 36 000 $M^{-1}cm^{-1}$).[55] From this stock solution, 250 µM aliquots were prepared and kept at -20 °C until use. All the peptides were bought from GeneCust (Dudelange, Luxembourg) with a purity grade > 98 %. Stock solutions of human $A\beta_{16}$ (sequence DAEFRHDSGYEVHHQK) were prepared at ca. 5 mM by dissolving the powder in ultrapure water, and their concentration was determined by UV-vis absorption of Tyr10 considered as free tyrosine (ε_{276}-ε_{296} = 1410 $M^{-1}cm^{-1}$). The human $A\beta_{40}$ peptide (sequence DAEFRHDSGYEVHHQKLVFFAEDVGSNKGAIIGLMVGGVV) was purified to obtain only a monomeric fraction prior its aggregation according to a previously reported protocol.[56] The peptide concentration was measured by UV-vis absorption of Tyr10 at basic pH (ε_{293}-ε_{360} = 2400 $M^{-1}cm^{-1}$). The shorter $A\beta_{16}$ peptide has been used for the experiments studying the coordination and the ROS production as a valuable model for Cu(II) binding to the full length peptide. The longer $A\beta_{40}$ peptide has been used for the experiments involving aggregation. No differences between the short and full-length hAβ peptides have been observed for their binding Cu(II) coordination, binding affinity or ROS production.[40,57]

X-Ray Absorption Near Edge Structure (XANES)

Zn-K edges XANES spectra were recorded on the FAME beamline at the European Synchrotron Radiation Facility (ESRF, Grenoble, France) during an 18-shifts session in April 2017 (Experiment number 30-02-1125). The measurements were performed on mM solutions at low temperature (He-cryostat) in the fluorescence mode using a 30-element high-purity Ge detector. The energy was calibrated by the measurement of Zn foil spectra in transmission. For each sample, at least 3 XANES spectra were recorded and averaged. Samples for XANES measurements were prepared in presence of 10% of glycerol as cryoprotectant.

Nuclear Magnetic Resonance (NMR)

NMR experiments were performed on an Avance 600 Bruker NMR spectrometer. All the reactant solutions were prepared in D_2O, and pH was adjusted with additions of D_2SO_4 or NaOD. Spectra were recorded at 298 K (for the methylene protons of PTA and its complex) or 318 K (aromatic protons of the peptide and its complexes). 318 K was chosen in order to obtain well

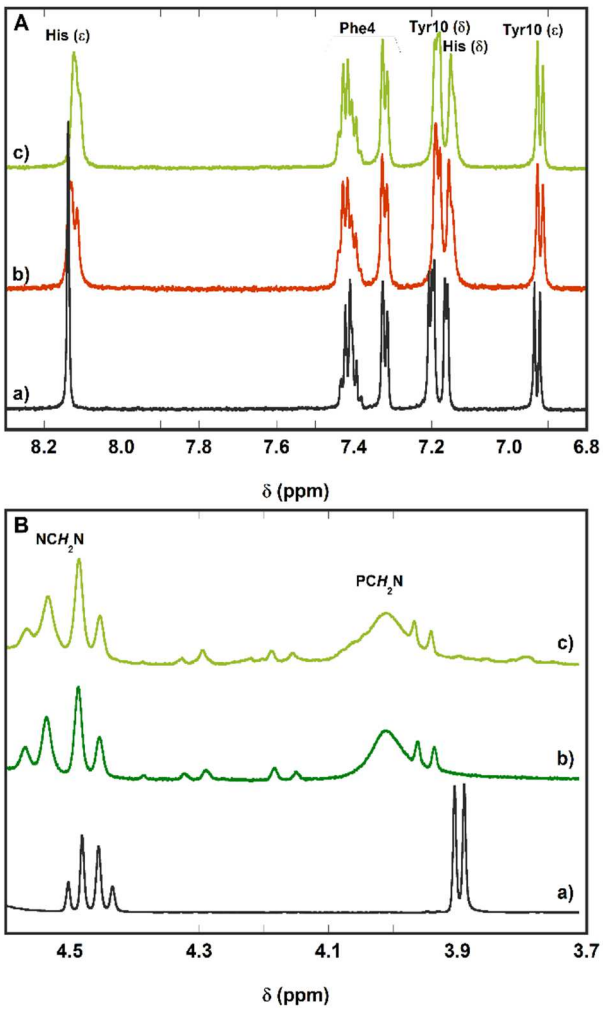

Figure 2. ^{1}H-NMR spectra at selected regions: panel **A**, aromatic region of a) $A\beta_{16}$, b) $Zn(A\beta_{16})$ complex, c) $Cu^{II},Zn^{II}(A\beta_{16})$ + 6 equivalent of PTA; panel **B**, methylene protons of a) PTA, b) Cu(II) + 6 equivalents of PTA, c) $Cu^{II},Zn^{II}(A\beta_{16})$ + 6 equivalents of PTA. Conditions: $[A\beta_{16}]$ = 300 µM, [Zn(II)] = [Cu(II)] = 270 µM, [PTA] = 1.8 mM, [Tris-d_{11}] = 50 mM, pH = 7.4, T = 318 K (**A**) and 298 K (**B**).

resolved peaks of the aromatic protons of the peptide. On the other hand, temperature was decreased for the spectra of the methylene protons of PTA since at 318 K the AB system of the NCH_2N protons was hindered by the signal of water.

UV-vis spectroscopy

UV-vis spectra were recorded on an Agilent 8453 UV-visible spectrometer, equipped with a Peltier temperature controller unit which maintained the solution temperature at 25 °C. For the kinetics of Cu(II) removal from the $Cu^{II},Zn(A\beta_{16})$ complex by PTA, the full spectra from 250 to 900 nm were recorded to study both the influence on the Tyr10 absorption band (280 nm) and the Cu(II) d-d band at 620 nm.

Ascorbate consumption

The spectra of consumption of ascorbate, which mirror the production of ROS,[37] were obtained by measuring the absorbance of ascorbate at 265 nm (ε = 14 500 $M^{-1}cm^{-1}$) with a correction at 800 nm as a function of time.

Thioflavin T assay

Kinetics of aggregation by the Thioflavin T (ThT) assay were recorded using a FLUOstar OPTIMA (BMG Labtech) plate reader. The experiments were prepared in 384-wells non-binding plates (Greiner BioOne) by dissolving the appropriate quantities of each reactant, in presence of ThT at 10 µM. 0.1 µM of EDTA was added (i.e.: 0.5% of [$A\beta_{40}$]) to sequestrate trace metal ions. We have control that EDTA has no effect on the aggregation of the Aβ peptide. ThT was excited at 440 nm and the emission was set at 490 nm. Three independent experiments were performed with three replicates for each condition.

Transmission Electron Microscopy (TEM)

Samples were taken after aggregation for 72 hours in the 384-well plates and collected by same conditions criteria. They were prepared for electron microscopy by using the conventional negative staining procedure. An aliquot (20 µL) of solution was absorbed on Formvar-carbon-coated grids for 2 min, blotted, and negatively stained with uranyl acetate (1%) for 1 min. Grids were examined with a TEM (Jeol JEM-1400, JEOL Inc, Pea- body, MA, USA) at 80 kV. Images were acquired by using a digital camera (Gatan Orius, Gatan Inc, Pleasanton, CA, USA) at 4000 or 25000 magnifications.

Results and discussion

Zn binding to PTA

XANES (X-ray Absorption Near Edge Structure) measurements were carried out to study the possible formation of a Zn(II)-PTA complex since it is the most suitable spectroscopic technique for Zn(II) which, due to its d^{10} electronic configuration, remains silent in most classical techniques. The complex [$ZnCl_2(PTA)_2$] had already been isolated by Smolenski et al.[58] as an air-stable solid product which undergoes ligand displacement in water. The formation of a Zn(II)-PTA complex is not observed in aqueous solution, as confirmed by XANES data (figure S1, a and b): the XANES spectrum of Zn(II) in buffer + 5 equivalents of PTA (b in figure S1) is virtually the same as Zn(II) in buffer (a in figure S1) at mM concentrations, thus indicating a very low affinity, at least lower than 10^3 M^{-1}, of PTA for Zn(II). This is the reason why PTA cannot compete with the peptide Aβ for binding Zn(II) (c in figure S1).

PTA keeps its ability to reduce and remove Cu from Aβ even in the presence of Zn(II)

The ability of PTA to reduce and remove Cu(II) from the Aβ peptide has been previously shown.[48] In this work, its ability has been tested also in the presence of Zn(II) which, as previously seen, can be found in the brain at higher concentration than copper. The very low affinity of PTA for Zn(II) leads to a good Cu-over-Zn selectivity overcoming that of Aβ as confirmed by ^{1}H-NMR spectroscopy (figure 2). Once PTA is added to a preformed solution of Cu^{II},Zn^{II}(Aβ), the ligand targets Cu(II) specifically to reduce it to Cu(I) and remove it from the peptide. In this process, Zn(II) remains bound to Aβ as it can be observed in figure 2, A: the aromatic protons of the peptide, and more specifically the histidine protons, recover the shift of the Zn(Aβ) complex after addition of 6 equivalents of PTA to the heteronuclear Cu^{II},Zn^{II}(Aβ). The formation of the $[Cu(PTA)_4]^+$ complex is confirmed by the downfield shift of the AB system of the NCH_2N protons of PTA (from 4.47 to 4.51) and the PCH_2N protons (from a defined doublet at 3.90 for uncoordinated PTA to a broad singlet at 4.01 for the $[Cu(PTA)_4]^+$

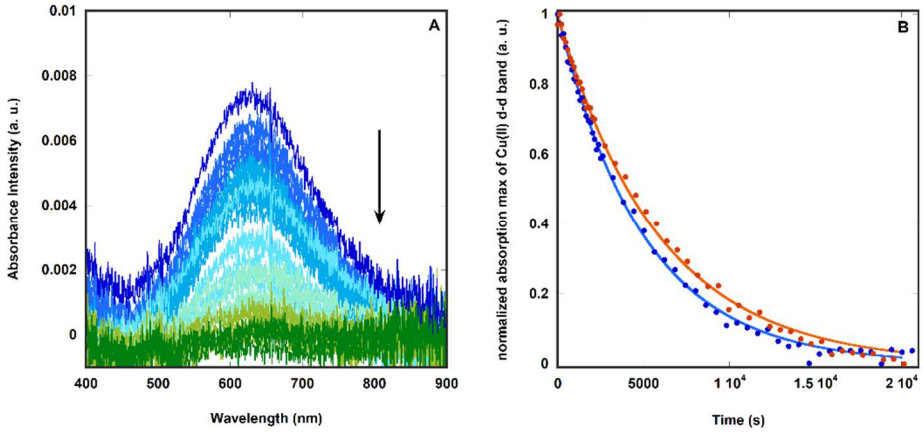

Figure 3. A) UV-Vis absorption spectra following the reduction of Cu(II) to Cu(I) by recording the Cu(II) d-d band over 5.5 h. Cu,Zn($A\beta_{16}$), dark blue line; Cu,Zn($A\beta_{16}$) + 5 equiv. PTA from 0 h (blue line) to 5.5 h (green line), measured every 120 s (0 → 2040 s) or 600 s (2040 → 20040 s). Conditions: [Cu(II)] = 90 µM, [$A\beta_{16}$] = 100 µM, [Zn(II)] = 90 µM, [PTA] = 500 µM, [HEPES] = 50 mM, pH 7.4. B) kinetic of the decrease of the maximum corresponding to the d-d band of the $Cu^{II}(A\beta_{16})$ (at 630 nm, blue dots) of Cu^{II},Zn($A\beta_{16}$) (at 620 nm, orange dots) complexes. Raw data of the absorbance from the UV-Vis spectra (left panel) have been averaged around the wavelength corresponding to the maximum of absorbance to eliminate noise due to the very low absorbance intensity. Data have been fitted to an exponential decay function ($Cu^{II}(A\beta_{16}$: blue line and Cu,Zn($A\beta_{16}$) : orange line).

complex).[48,59] PTA oxide is formed as a by-product of the reduction of Cu(II) to Cu(I)[48] and it can be observed in the spectra of the reactions Cu(II) + 6 equiv. of PTA (b in figure 2B) and Cu^{II},Zn^{II}(Aβ) + 6 equiv. of PTA (c in figure 2B). The AB system of PTA oxide is centred at 4.23, while the PCH_2N protons appear as a doublet at 3.95.

The low affinity of PTA for Zn(II) confers this ligand a very good Cu-over-Zn selectivity, overcoming that of Aβ. Indeed, the presence of Zn(II) does not impede PTA to reduce Cu(II) bound to the peptide and remove it to form the $[Cu(PTA)_4]^+$ complex, leaving Zn(II) still coordinated to Aβ (Scheme 1).

The rate of Cu(II) to Cu(I) reduction by PTA in presence or absence of Zn(II) has also been studied by following the Cu(II)-characteristic d-d band at 620 nm (figure 3, A). This study also allows the monitoring of the time needed to reduce copper and if the addition of zinc alters the kinetic of the reduction. Data obtained were fitted to an exponential decay function characteristic of first-order reactions (equation 1).

$$y = y_0 e^{-kx}$$

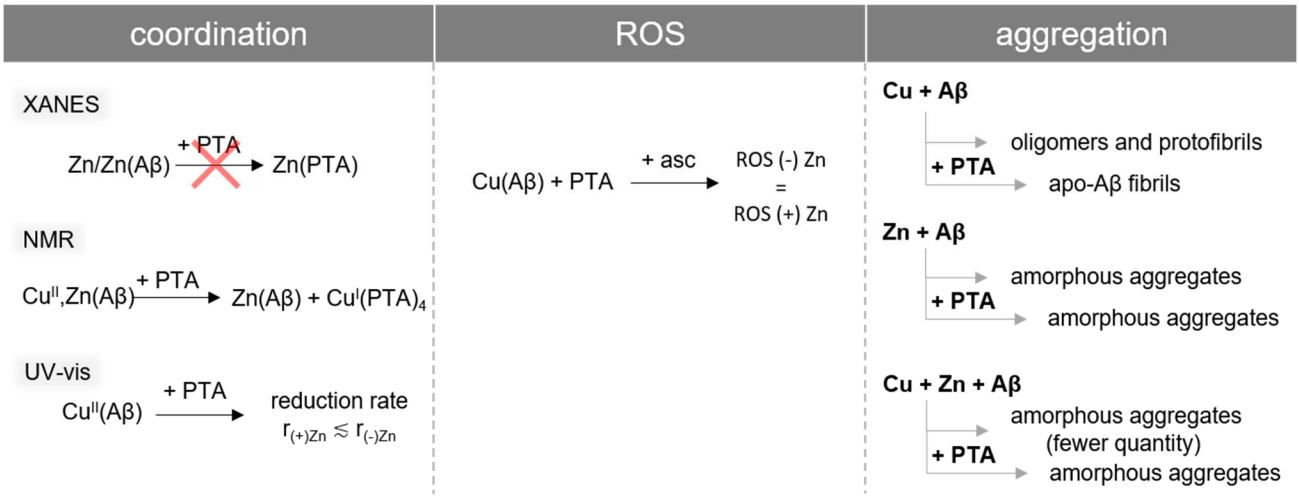

Scheme 1. Summary of the reactions taking place with Cu and Zn complexes with the Aβ peptide with or without PTA.

Equation 1. Exponential decay function where x = time (s), y = normalized absorption max (a. u.) and k = reduction rate constant (s^{-1}).

In presence of Zn(II) the reduction of Cu(II) to Cu(I) is slightly slower: $k_{(-)Zn}$ = 2.0 x 10^{-4} s^{-1} *vs.* $k_{(+)Zn}$ = 1.7 x 10^{-4} s^{-1} (figure 3, B) in line with the displacement of Cu(II) to its coordination mode II (figure 1) in the heteronuclear complex Cu^{II},Zn^{II}(Aβ),[7,37,38,60] which is expected to be more difficult to reduce. Nevertheless, this slightly slower rate does not hamper the overall reduction and removal of copper process. Indeed, after fours hours and in presence of 5 equivalents of PTA at [Cu(II)] = 90 µM (Figure 3, B), most of Cu(II) is reduced regardless the presence of zinc (Scheme 1). PTA has a higher selectivity for copper over zinc than Aβ as demonstrated by these results. Therefore, the presence of Zn(II) in solution does not prevent PTA from reducing Cu(II) to Cu(I) and subtracting it from the peptide.

The presence of Zn(II) does not impact the formation of $[Cu(PTA)_4]^+$ in a ROS-forming reaction

Then, the effect of PTA on ROS production by Cu(Aβ) was probed in absence and presence of Zn(II).

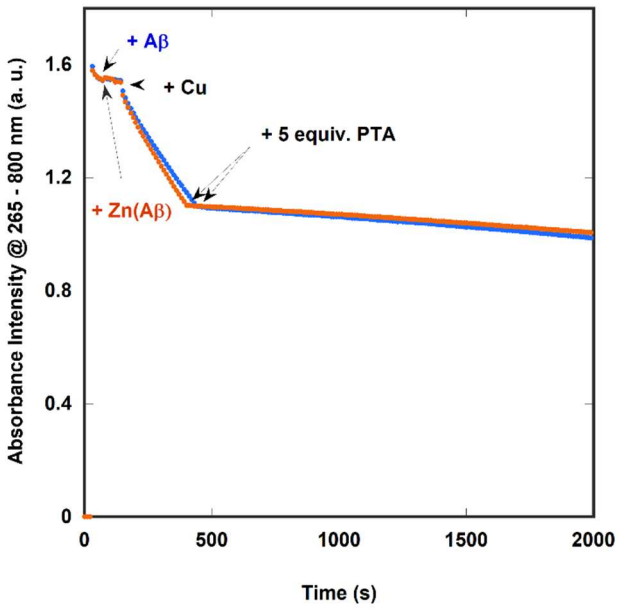

Figure 4.UV-Vis absorption of ascorbate (followed at λ_{max} = 265 nm) as a function of time in presence of Cu($A\beta_{16}$) (blue dots) and Cu,Zn($A\beta_{16}$) (orange dots) and after addition of 5 equivalents of PTA. Conditions: [Cu(II)] = [Zn(II)] = 10 µM, [$A\beta_{16}$] = 12 µM, [PTA] = 60 µM, [ascorbate] = 100 µM, [HEPES] = 50 mM, pH 7.4, T = 25 °C.

The redox activity of the mono- and dinuclear peptide complexes was followed by the consumption of ascorbate, which is a biologically relevant reductant. Monitoring of the ascorbate consumption at 265 nm mirrors the production of ROS because ascorbate performs the reduction of Cu(Aβ) that, in turn, reduces O_2 to $O_2^{\bullet-}$, H_2O_2 and $HO^{\bullet}$.[19] The mixed-metal complex has indeed a slightly higher ascorbate oxidation rate than the monometallic complex Cu(Aβ) (figure 4) as already reported.[61] In this case, regardless the presence of Zn(II) and its enhancement for ROS production, 5 equiv. of PTA do effectively arrest the ROS production by Cu bound to Aβ (Figure 4 and Scheme 1).

PTA can prevent Cu-induced oligomerisation of the Aβ peptide even in the presence of Zn(II)

PTA previously showed to be effective avoiding the formation of Cu(Aβ) oligomers and restoring the formation of apo-like amyloid fibrils.[48] In this work, its ability has been also tested in presence of Zn(Aβ) and the heteronuclear complex Cu,Zn(Aβ). First, the impact of 5 and 20 equivalents of PTA on Cu(Aβ) aggregation were evaluated (Figure 5, panel A and Figure S2, panel A). Under the conditions used in the present study apo-Aβ exhibits a sigmoid-like curve in the ThT fluorescence experiment, where ThT

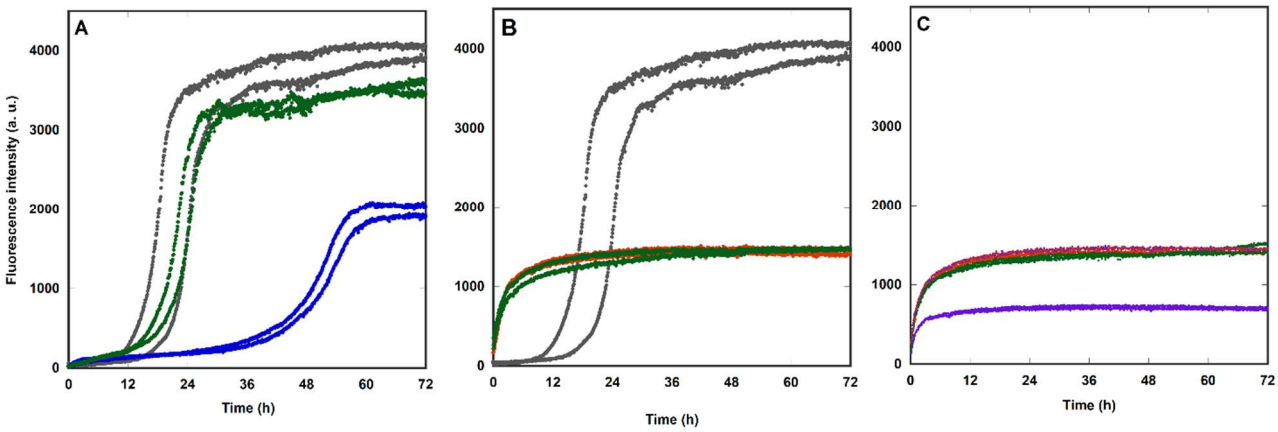

Figure 5. ThT-fluorescence spectra as a function of time of the aggregation of $A\beta_{40}$ in presence of (**A**) Cu(II), (**B**) Zn(II) and (**C**) Cu(II) + Zn(II); and the effect of adding 20 equivalents of PTA. [$A\beta_{40}$] = 20 µM, [Cu(II)] = [Zn(II)] = 18 µM, [PTA] = 400 µM, [ThT] = 10 µM, [NaCl] = 100 mM, [EDTA] = 0.1 µM, [HEPES] = 50 mM, pH 7.4, T = 37 °C. Colour code of curves: (**A**) a) grey, apo-Aβ; b) blue, Cu(Aβ); c) green, Cu(Aβ) + PTA; (**B**) d) grey, apo-Aβ; e) orange, Zn(Aβ); f) green, Zn(Aβ) + PTA; (**C**) g) orange, Zn(Aβ); h) purple, Cu,Zn(Aβ); i) green, Cu,Zn(Aβ) + PTA.

is a dye that acquires a strong fluorescence upon interaction with β-sheets structures, thus mirroring the formation of β-sheets.[62] In the presence of up to 0.9 equiv. of Cu(II), the sigmoid-like curve is conserved but the start of the aggregation is delayed and the intensity reached at the plateau is ca. half of that observed for the apo-fibrils. This is in line with the aggregates observed by TEM (Fig. S3), since shorter fibres are formed and in less quantity. Addition of 20 equivalents of PTA leads to the recovery of the sigmoid curve and morphology of the apo-peptide fibrils. This recovery is only partial in the case of addition of 5 equivalents of PTA (Fig. S2 & S3) due to the partial oxidation of PTA to overcome the reoxidation of Cu(II) when there is not enough reductant in the medium. This is in line with what was observed and discussed in our previous work.[48] Furthermore, consistent with the low affinity of PTA for Zn(II), the addition of PTA to the Zn($A\beta_{40}$) solution does not change either the aggregation curve nor the aggregates formed: indeed, in presence of 0.9 equivalents of Zn(II), with or without PTA, an initial acceleration of the aggregation process is observed and after less than 12 hours a plateau is reached, of approximately 35% of the intensity of the apo-peptide (Fig. 5, panel B). Furthermore, the morphology of the aggregates formed in presence of Zn(II) could be described as amorphous aggregates (Fig. S3) in line with previous reports.[13,63,64] When the aggregation experiment is run in presence of 0.9 equivalents of both Cu(II) and Zn(II), a similar curve to that observed for the Zn($A\beta_{40}$) complex is obtained but with a lower final intensity (Fig. 4, panel C). The morphology of the aggregates relates as well to the Zn(II) complex (Fig. S3). In accordance to literature,[18] Zn(II) dominates the aggregation process but the presence of Cu(II) leads to lower intensity ThT signal. Addition of 20 equivalents of PTA leads to a ThT-curve and TEM images which are very similar to those of the Zn($A\beta_{40}$) complex. Therefore, the presence of Zn(II) does not preclude the removal of Cu(II) from the peptide by PTA and its addition could prevent the formation of more toxic aggregates such as Cu-induced oligomers. Contrary to what is observed after the addition of only 5 equivalents of PTA to the Cu(Aβ) complex, 5 equivalents are enough to sequestrate Cu(II) from Aβ when in presence of Zn(II) and obtain a curve similar to that of the Zn(Aβ) complex (Fig. S2). We anticipate that the formation of insoluble Zn(Aβ) aggregates facilitates the formation of the redox silent $[Cu(PTA)_4]^+$ complex in solution. In brief, the presence of Zn does not preclude the removal of Cu(II) from Aβ by the PTA ligand and induces the formation of Zn-type aggregates.

Discussion and concluding remarks

As noted in the Introduction, the speciation of the $[Cu(PTA)_n]^+$ complex changes depending on the Cu:PTA stoichiometry, the concentration and the other molecules present in the reaction medium. In the conditions of the experiments described in this work, both $[Cu(PTA)_2]^+$ and $[Cu(PTA)_3]^+$ have been proposed to be predominant in solution.[48,50,51] Quaretti et al.[51] hypothesised that, in presence of Aβ, the prevalence of the $[Cu(PTA)_2]^+$ species could lead to the formation of ternary species such as $[Cu(PTA)_2(Aβ)]$, in line with the ternary complexes formed with PTA and the aromatic bidentate ligands BCA (2,2'-biquinoline-4,4'-carboxylic acid) and i-BCS (bathocuproinedisulfonic acid). Contrary to this theory, the NMR spectra shown here, together with the XANES spectra previously reported,[48] do not show the formation of a ternary Cu(I)-Aβ-$(PTA)_2$ species. This may be due to the linear binding mode of Cu(I) by the Aβ peptide that would not easily accommodate the tetrahedral geometry of such ternary species, in contrast to what is observed with the BCS or BCA ligands.[51]

To sum up, we show in this work how PTA maintains its effectiveness to remove Cu ions from the Aβ peptide even in the presence of highly-concentrated Zn(II). In fact, a Cu-over-Zn selectivity greater than that of Aβ should be one of the required characteristics for metal-targeting ligands as potential drug candidates in the treatment of AD as previously demonstrated for Cu(II).[7] The here described proof-of-concept idea could be a key point to overcome the failure of metal-targeting molecules in clinical trials of AD. As presented in the introduction, a soft base atom such as P in the case of PTA, will show a greater affinity for Cu(I) than for Zn(II) satisfying the Cu-over-Zn selectivity criteria. Therefore, playing with the electronic properties of the ligand might be enough for Cu(I)-targeting ligands, while other structural parameters should be considered as well for Cu(II)-targeting ligands. This will be of importance when translating these requirements into drugs with potential clinical use due to the complexity of the biological environment.

Another interesting point is that Ceresa et al.[66] have demonstrated that the anti-cancerous $[Cu(PTA)_4]PF_6$ complex is not neurotoxic at concentrations higher than its IC_{50} value in human cancer cells. In addition, the complex can enter neurons without exerting any *in vivo* deleterious effects.[66] This could be interesting to restore a normal homeostasis of copper in the brain, another key point when developing therapeutic metal-targeting drugs aimed at restoring normal Cu homeostasis in the brain.[67,68]

Conflicts of interest

There are no conflicts to declare.

Acknowledgements

This research is supported by the European Research Council (StG-638712, granted to Dr. Hureau). The authors also thank Vanesa Soldan and the service of Genotoul TRI at Toulouse for their assistance in TEM and Christian Bijani for acquiring the NMR spectra. The authors acknowledge the European Synchrotron Radiation Facility for provision of beamtime (experiment 30-02-1125), and the FAME staff for their support.

Notes and references

1 Alzheimer's Dement. J. Alzheimer's Assoc., 2017, **13**, 325–373.
2 J. Hardy and D. J. Sekoe, *Science*, 2002, **297**, 353–356.
3 C. Hureau, *Coord. Chem. Rev.*, 2012, **256**, 2164–2174.
4 E. Atrián-Blasco, P. González, A. Santoro, B. Alies, P. Faller and C. Hureau, *Coord. Chem. Rev.*, 2018, **371**, 38–55.
5 M. A. Lovell, J. D. Robertson, W. J. Teesdale, J. L. Campbell and W. R. Markesbery, *J. Neurol. Sci.*, 1998, **158**, 47–52.
6 X. Huang, C. S. Atwood, R. D. Moir, M. A. Hartshorn, R. E. Tanzi and A. I. Bush, *J. Biol. Inorg. Chem.*, 2004, **9**, 954–960.
7 E. Atrián-Blasco, A. Conte-Daban and C. Hureau, *Dalton Trans.*, 2017, **46**, 12750–12759.
8 F. Bousejra-ElGarah, C. Bijani, Y. Coppel, P. Faller and C. Hureau, *Inorg. Chem.*, 2011, **50**, 9024–9030.
9 K. L. Stewart and S. E. Radford, *Biophys. Rev.*, 2017, **9**, 405–419.
10 F. Hane and Z. Leonenko, *Biomolecules*, 2014, **4**, 101–116.
11 J. T. Pedersen, K. Teilum, N. H. H. Heegaard, J. Østergaard, H.-W. Adolph and L. Hemmingsen, *Angew. Chemie Int. Ed.*, 2011, **50**, 2532–2535.
12 C. J. Matheou, N. D. Younan and J. H. Viles, *Biochem. J.*, 2015, **466**, 233–242.
13 A. K. Sharma, S. T. Pavlova, J. Kim, J. Kim and L. M. Mirica, *Metallomics*, 2013, **5**, 1529–1536.
14 Y. Yoshiike, K. Tanemura, O. Murayama, T. Akagi, M. Murayama, S. Sato, X. Sun, N. Tanaka and A. Takashima, *J. Biol. Chem.*, 2001, **276**, 32293–32299.
15 B. Raman, T. Ban, K. I. Yamaguchi, M. Sakai, T. Kawai, H. Naiki and Y. Goto, *J. Biol. Chem.*, 2005, **280**, 16157–16162.
16 V. Tõugu, A. Karafin, K. Zovo, R. S. Chung, C. Howells, A. K. West and P. Palumaa, *J. Neurochem.*, 2009, **110**, 1784–1795.
17 L. Pan and J. C. Patterson, *PLoS ONE*, 2013, **8**, e70681.
18 C. J. Matheou, N. D. Younan and J. H. Viles, *J. Mol. Biol.*, 2016, **428**, 2832–2846.
19 C. Cheignon, M. Tomas, D. Bonnefont-Rousselot, P. Faller, C. Hureau and F. Collin, *Redox Biol.*, 2018, **14**, 450–464.
20 M. G. Savelieff, G. Nam, J. Kang, H. J. Lee, M. Lee and M. H. Lim, *Chem. Rev.*, 2019, **119**, 1221–1322.
21 M. E. Rice, *Trends Neurosci.*, 2000, **23**, 209–216.
22 F. E. Harrison and J. M. May, *Free Radic. Biol. Med.*, 2009, **46**, 719–730.
23 G. Multhaup, A. Schlicksupp, L. Hesse, D. Beher, T. Ruppert, C. L. Masters and K. Beyreuther, *Science*, 1996, **271**, 1406–1409.
24 J. S. McDowall and D. R. Brown, *Metallomics*, 2016, **8**, 385–397.
25 K. J. Barnham and A. I. Bush, *Chem. Soc. Rev.*, 2014, **43**, 6727–6749.
26 E. I. Solomon, D. E. Heppner, E. M. Johnston, J. W. Ginsbach, J. Cirera, M. Qayyum, M. T. Kieber-Emmons, C. H. Kjaergaard, R. G. Hadt and L. Tian, *Chem. Rev.*, 2014, **114**, 3659–3853.
27 N. Horn, L. B. Møller, V. M. Nurchi and J. Aaseth, *J. Inorg. Biochem.*, 2019, **190**, 98–112.
28 N. D'Ambrosi and L. Rossi, *Neurochem. Int.*, 2015, **90**, 36–45.
29 B. Alies, E. Renaglia, M. Rózga, W. Bal, P. Faller and C. Hureau, *Anal. Chem.*, 2013, **85**, 1501–1508.
30 T. R. Young, A. Kirchner, A. G. Wedd and Z. Xiao, *Metallomics*, 2014, **6**, 505–517.
31 B. Alies, A. Conte-Daban, S. Sayen, F. Collin, I. Kieffer, E. Guillon, P. Faller and C. Hureau, *Inorg. Chem.*, 2016, **55**, 10499–10509.
32 S. Noël, S. Bustos Rodriguez, S. Sayen, E. Guillon, P. Faller and C. Hureau, *Metallomics*, 2014, **6**, 1220–1222.
33 J. Shearer and V. A. Szalai, *J. Am. Chem. Soc.*, 2008, **130**, 17826–17835.
34 C. Hureau, V. Balland, Y. Coppel, P.-L. Solari, E. Fonda and P. Faller, *J. Biol. Inorg. Chem.*, 2009, **14**, 995–1000.
35 B. Alies, B. Badei, P. Faller and C. Hureau, *Chem. Eur. J.*, 2012, **18**, 1161–1167.
36 N. Yako, T. R. Young, J. M. Cottam Jones, C. A. Hutton, A. G. Wedd and Z. Xiao, *Metallomics*, 2017, **9**, 278–291.
37 B. Alies, I. Sasaki, O. Proux, S. Sayen, E. Guillon, P. Faller and C. Hureau, *Chem. Commun.*, 2013, **49**, 1214–1216.
38 C. A. Damante, K. Ösz, Z. Nagy, G. Grasso, G. Pappalardo, E. Rizzarelli and I. Sóvágó, *Inorg. Chem.*, 2011, **50**, 5342–5350.
39 V. Balland, C. Hureau and J.-M. Savéant, *Proc. Natl. Acad. Sci. U.S.A.*, 2010, **107**, 17113–17118.
40 C. Cheignon, M. Jones, E. Atrián-Blasco, I. Kieffer, P. Faller, F. Collin and C. Hureau, *Chem. Sci.*, 2017, **8**, 5107–5118.
41 P. Faller, C. Hureau, *Dalton Trans.*, 2009, 1080-1084
42 S. A. James, I. Volitakis, P. A. Adlard, J. A. Duce, C. L. Masters, R. A. Cherny and A. I. Bush, *Free Radic. Biol. Med.*, 2012, **52**, 298–302.
43 A. Robert, Y. Liu, M. Nguyen and B. Meunier, *Acc. Chem. Res.*, 2015, **48**, 1332–1339.
44 C. J. Frederickson, *Int. Rev. Neurobiol.*, 1989, **31**, 145–238.
45 D. E. Hartter and A. Barnea, *J. Biol. Chem.*, 1988, **263**, 799–805.
46 J. Kardos, L. Héja, A. Simon, I. Jablonkai, R. Kovacs and K. Jemnitz, *Cell Comm. Sign.* 2018, 16, 71
47 R. G. Pearson, *J. Am. Chem. Soc.*, 1963, **85**, 3533–3539.
48 E. Atrián-Blasco, E. Cerrada, A. Conte-Daban, D. Testemale, P. Faller, M. Laguna and C. Hureau, *Metallomics*, 2015, **7**, 1229–1232.
49 A. Guerriero, M. Peruzzini and L. Gonsalvi, *Coord. Chem. Rev.*, 2018, **355**, 328–361.

50 F. Endrizzi, P. Di Bernardo, P. L. Zanonato, F. Tisato, M. Porchia, A. A. Isse, A. Melchior and M. Tolazzi, *Dalton Trans.*, 2017, **46**, 1455–1466.
51 M. Quaretti, M. Porchia, F. Tisato, A. Trapananti, G. Aquilanti, M. Damjanović, L. Marchiò, M. Giorgetti and M. Tegoni, *J. Inorg. Biochem.*, 2018, **188**, 50–61.
52 W. P. Walters, Expert Opin. Drug. Discov. 2012, **7**, 99-107.
53 F. Jianghong, I. A. M. de Lannoy, *Biochem. Pharmacol.*, 2014, **87**, 93-120.
54 D. J. Daigle, *Inorg. Synth.*, 1998, **32**, 40–45.
55 M. Groenning, L. Olsen, M. van de Weert, J. M. Flink, S. Frokjaer and F. S. Jørgensen, *J. Struct. Biol.*, 2007, **158**, 358–369.
56 A. Conte-Daban, V. Ambike, R. Guillot, N. Delsuc, C. Policar and C. Hureau, *Chem. Eur. J.*, 2018, **24**, 5095–5099.
57 V. Minicozzi, F. Stellato, M. Comai, M. Dalla Serra, C. Potrich, W. Meyer-Klaucke and S. Morante, *J. Biol. Chem.*, 2008, **283**, 10784–10792.
58 P. Smoleński, L. Benisvy, M. F. C. G. Da Silva and A. J. L. Pombeiro, *Eur. J. Inorg. Chem.*, 2009, **2**, 1181–1186.
59 A. M. Kirillov, P. Smoleński, M. F. C. G. Da Silva and A. J. L. Pombeiro, *Eur. J. Inorg. Chem.*, 2007, 2686–2692.
60 K. I. Silva and S. Saxena, *J. Phys. Chem. B*, 2013, **117**, 9386–9394.
61 E. Atrián-Blasco, M. del Barrio, P. Faller and C. Hureau, *Anal. Chem.*, 2018, **90**, 5909–5915.
62 S. Noël, S. Cadet, E. Gras and C. Hureau, *Chem. Soc. Rev.*, 2013, **42**, 7747–7762.
63 D. Noy, I. Solomonov, O. Sinkevich, T. Arad, K. Kjaer and I. Sagi, *J. Am. Chem. Soc.*, 2008, **130**, 1376–1383.
64 A. I. Bush, W. H. Pettingell, G. Multhaup, M. D. Paradis, J.-P. Vonsattel, J. F. Gusella, K. Beyreuther, C. L. Masters and R. E. Tanzi, *Science*, 1994, **265**, 1464–1467.
65 C. Ha, J. Ryu, C. B., Park, *Biochemistry*, 2007, **20**, 6118-6125.
66 C. Ceresa, G. Nicolini, S. Semperboni, V. Gandin, M. Monfrini, F. Avezza, P. Alberti, A. Bravin, M. Pellei, C. Santini and G. Cavaletti, *Neurotox. Res.*, 2018, 10.1007/s12640-018-9864-8.
67 E. M. Andreozzi, J. Baguña Torres, K. Sunassee, J. Dunn, S. Walker-Samuel, I. Szanda and P. J. Blower, *Metallomics*, 2017, **9**, 1622–1633.
68 Z. K. Mathys and A. R. White, in *Neurotoxicity of Metals*, eds. M. Aschner and L. G. Costa, Springer International Publishing, Cham, 2017, pp. 199–216.